Synthesis and Dielectric Properties of Polystyrene–Clay Nanocomposite Materials

Hong-Wen Wang, Kung-Chin Chang, Jui-Ming Yeh, Shir-Joe Liou

Department of Chemistry and Center for Nanotechnology at CYCU, Chung-Yuan Christian University, ChungLi 320, Taiwan, Republic of China

Received 10 March 2003; accepted 16 June 2003

ABSTRACT: Polystyrene–clay nanocomposite (PsCN) materials were synthesized and their properties of crystallinity, thermal behavior, and dielectric characteristics were investigated. A polymerizable cationic surfactant, [2-(dimethylamino)ethyl]triphenylphonium bromide, was used for the intercalation of montmorillonite (MMT). The organophilic MMT was prepared by Na^+-exchanged MMT and ammonium cations of a cationic surfactant in an aqueous medium. Organophilic styrene monomers were intercalated into the interlayer regions of organophilic clay hosts followed by a free-radical polymerization. Exfoliation to 2 wt % MMT in the polystyrene (PS) matrix was achieved as revealed by X-ray diffraction (XRD) and transmission electron microscopy (TEM). Thermal properties by differential scanning calorimetry (DSC) and thermogravimetric analysis (TGA) were also studied. The dielectric properties of PsCNs in the form of film with clay loading from 1.0 to 5.0 wt % were measured under frequencies of 100 Hz–1 MHz at 25–70°C. A decreased dielectric constant and low dielectric loss were observed for PsCN materials. The dielectric response at low frequency that originated from dipole orientation was suppressed due to the intercalation of clay materials. © 2003 Wiley Periodicals, Inc. J Appl Polym Sci 91: 1368–1373, 2004

Key words: polystyrene; clay; nanocomposites; dielectric properties

INTRODUCTION

Polymer composite materials are widely used in areas such as electronics, transportation, construction, and consumer products. However, polymer–clay nanocomposite materials have been extensively studied in recent years. When compared to pristine polymers, polymer–clay nanocomposites possess many desirable properties, such as enhanced gas barriers, fire retardance, corrosion resistance, and ionic conductivities, increased thermal stability and mechanical strength, and decreased absorption in organic liquids.[1–4]

Polymer–clay nanocomposites are typically composed of an organically modified clay and polymer. The clay that is most commonly used is montmorillonite (MMT, a smectite clay),[5] which is an aluminosilicate mineral with sodium counterions present between the clay layers. To make this compatible with organic polymers, the sodium counterions are usually ion-exchanged with an organic ammonium or phosphonium salt to convert this material into a hydrophobic ammonium- or phosphonium-treated clay.[6]

Several attempts to prepare polystyrene–clay nanocomposites (PsCNs) have been reported. A common technique involves impregnating clay in a styrene monomer followed by polymerization. Intercalated PsCNs have been prepared by several researchers. Kato et al.[7] reported the intercalation of polystyrene (PS) in stearyltrimethylammonium cation-exchanged MMT. Kelly et al.[8,9] reported the modification of MMT by a variety of functional groups in their study of epoxy composites. Akelah and Moet[10,11] prepared PS nanocomposites using a solvent (acetonitrile). Recently, Doh and Cho[12] reported the synthesis of intercalated PS–MMT nanocomposites by *in situ* polymerization of styrene-containing dispersed organophilic MMT.[13–15] The dielectric properties of polymer–clay nanocomposites have been ignored in research. We start from the PS–clay system, since its synthesis and properties are well known, but its dielectric properties have not been studied in detail yet.

In the present investigation, the intercalation of cation-exchanged MMT using [2-(dimethylamino)ethyl]triphenylphonium bromide was synthesized. The structure of the PsCNs was characterized by Fourier transform infrared spectroscopy (FTIR), wide-angle powder X-ray diffraction (WAXD), and transmission electron microscopy (TEM). The thermal stability and dielectric behaviors of these nanocomposites were investigated.

Correspondence to: H.-W. Wang (hongwen@cycu.edu.tw).
Contract grant sponsor: NSC; contract grant number: 91-2113-M-033-008.

Journal of Applied Polymer Science, Vol. 91, 1368–1373 (2004)

EXPERIMENTAL

Materials

The MMT, with a cation-exchange capacity (CEC) of 98 mequiv/100 g, was supplied by the Pai Kong Co. (Taoyuan, Taiwan). [2-(Dimethylamino)ethyl]triphenylphonium bromide, (Aldrich, Milwaukee, WI, 97.0%), was used as an intercalating agent. Styrene was purchased from Fluka Chemical and benzoyl peroxide (Fluka, Buchs, Switzerland, 97%) was used as a free-radical initiator. Tetrahydrofuran (Mallinckrodt, USA, 99%), methanol (Mallinckrodt, 99.8%), hydrochloric acid (Riedel-de Haen, 37 %), and *N*-methyl-2-pyrrolidinone (Mallinckrodt, 99.0 %) were used as received.

Preparation of organoplilic clay[2,3]

The organophilic clay was prepared by a cation-exchange method, which is a reaction between the sodium cations of MMT clay and the alkyl ammonium ions of an intercalation agent. Typically, 5 g of MMT clay with a CEC value of 98 mequiv/100 g was stirred in 600 mL of distilled water (beaker A) at room temperature overnight. A separate solution containing 2.4 g of an intercalating agent in another 30 mL of distilled water (beaker B) under magnetic stirring, followed by adding a 1.0*M* HCl aqueous solution to adjust the pH value to about 3–4, was prepared. After stirring for 3 h, the protonated amino acid solution (beaker B) was added at a rate of approximately 10 mL/min with vigorous stirring to the MMT suspension (beaker A).[16] The mixture was stirred overnight at room temperature. The organophilic clay was recovered by ultracentrifugating (9000 rpm, 30 min) and filtering the solution in a Buchner funnel. Purification of the products was performed by washing and filtering samples repeatedly at least four times to remove any excess of ammonium ions. Organophilic clay was thus obtained.

Preparation of PsCNs

An appropriate amount of organophilic clay (0.1 g) was introduced into 100 mL of tetrahydrofuran under magnetic stirring overnight at room temperature. The styrene monomer, 9.9 g, was subsequently added to the solution, which was stirred for another 24 h. Upon addition of benzoyl peroxide (0.115 g), the solution was stirred for 24 h at 85°C under a N_2 atmosphere. The as-synthesized lamellar nanocomposite precipitates were then obtained by precipitating from an excess amount of methanol (500 mL) and subsequent drying under a dynamic vacuum at room temperature for 48 h.

Characterization of nanocomposites

A WAXD study of the samples was performed on a Rigaku D/MAX-3C OD-2988N X-ray diffractometer with a copper target and a Ni filter at a scanning rate of 2°/min. The decrease of the 2θ diffraction angles indicates an expansion of layer spacing of the clay materials. The absence of a diffraction peak for the PsCN materials may result from, first, a low content of clay and, second, complete exfoliation of the clay materials. For the second case, TEM observation is required. The samples for the TEM study were taken from a microtomed section of PsCNs, which were 60–90 nm in thickness and mounted in a resin. A TEM (JEOL-200FX) with an acceleration voltage of 120 kV was employed for the observation. FTIR spectra were obtained at a resolution of 4.0 cm^{-1} with an FTIR (BIO-RAD FTS-7) at room temperature ranging from 4000 to 400 cm^{-1}. The FTIR spectra provided further evidence that both materials (PS and clay) were intercalated.

Thermal gravimetric analysis (TGA) was performed on a Mettler–Toledo TGA/SDTA851 thermal analysis system in an air atmosphere. The heating rate was 20°C/min, and the temperature range was from 30 to 800°C. Differential scanning calorimetry (DSC) was performed on a Perkin–Elmer DSC-7 at a heating or cooling rate of 10°C/min in a nitrogen atmosphere. The temperature range was from 25 to 150°C. The glass transition temperature (T_g) of PS and the PsCN materials was recorded based on the second scanning. Dielectric parameters such as the capacitance and dissipation factor (tan δ) were measured by a Zentech 3305 automatic component analyzer at various frequencies (100 Hz to 1 MHz) under temperatures of 25–75°C. Above 75°C, PsCN specimens softened and measurement could not be well characterized. A vacuum-evaporated aluminum electrode was deposited on both sides of the nanocomposite film (area 1.5 cm in diameter). The thickness of samples was 70–90 μm.[17] The dielectric constant (ε_r) of the specimens was calculated by the equation $C = \varepsilon_r\ \varepsilon_0\ (A/d)$. ε_0 is the vacuum permittivity and equals 8.85×10^{-12} F/m. A is the electrode area, and d, the thickness of the specimen.

RESULTS AND DISCUSSION

X-ray diffraction

Figure 1 shows the WAXD patterns for organophilic clay and a series of PsCN materials. The d_{001} spacing was calculated from peak positions using Bragg's law: $n\lambda = 2d \sin\theta$, where λ is the X-ray wavelength (1.5418 Å). For organophilic clay and PsCN materials, the diffraction peaks in $2\theta = 2$–10° were recorded. The d_{001} spacing of vacuum-dried pristine MMT clay was 1.21 nm ($2\theta = 7.3°$). After the cation exchange, the d_{001} space increased to 1.88 nm ($2\theta = 4.7°$), as shown in the organophilic clay of Figure 1. Figure 1 also shows a lack of any diffraction peaks for the PS–clay 1% and

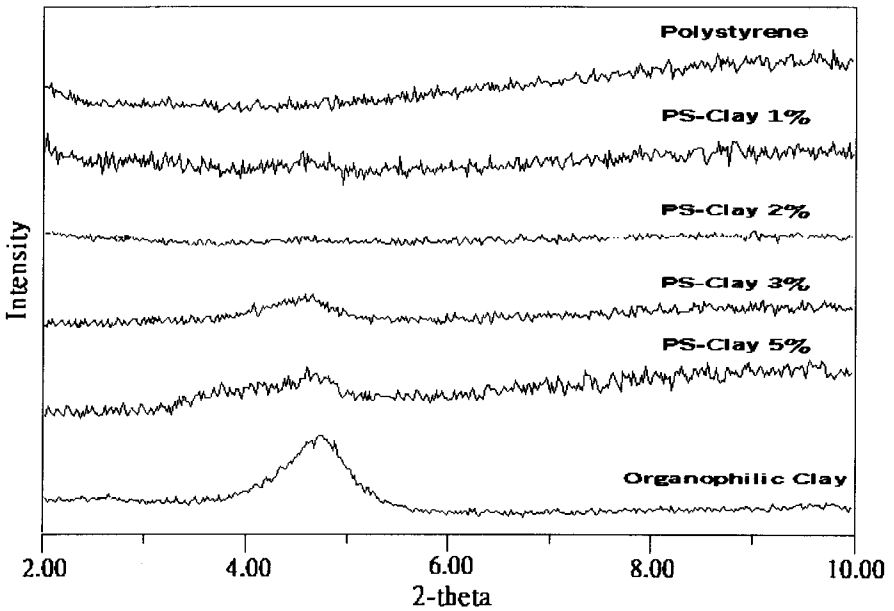

Figure 1 WAXD patterns of organophilic clay, PS, and a series of PsCN materials.

PS–clay 2%, indicating a complete exfoliation situation. When the amount of organoclay increased to 3.0 wt %, there was a small peak appearing at $2\theta = 4.5°$, corresponding a d spacing of 1.96 nm. This implied that there is a small amount of organoclay that could not be exfoliated in the PS and existed in the form of an intercalated layer structure.

FTIR

Figure 2 shows FTIR spectra of PS and a series of the PsCN materials. Table I illustrates the infrared band assignments of PS and MMT clay. The characteristic vibration bands of PS are at 1450, 1500, and 1600 cm^{-1} (aromatic C═C), 700 and 750 cm^{-1} (monosubstituted

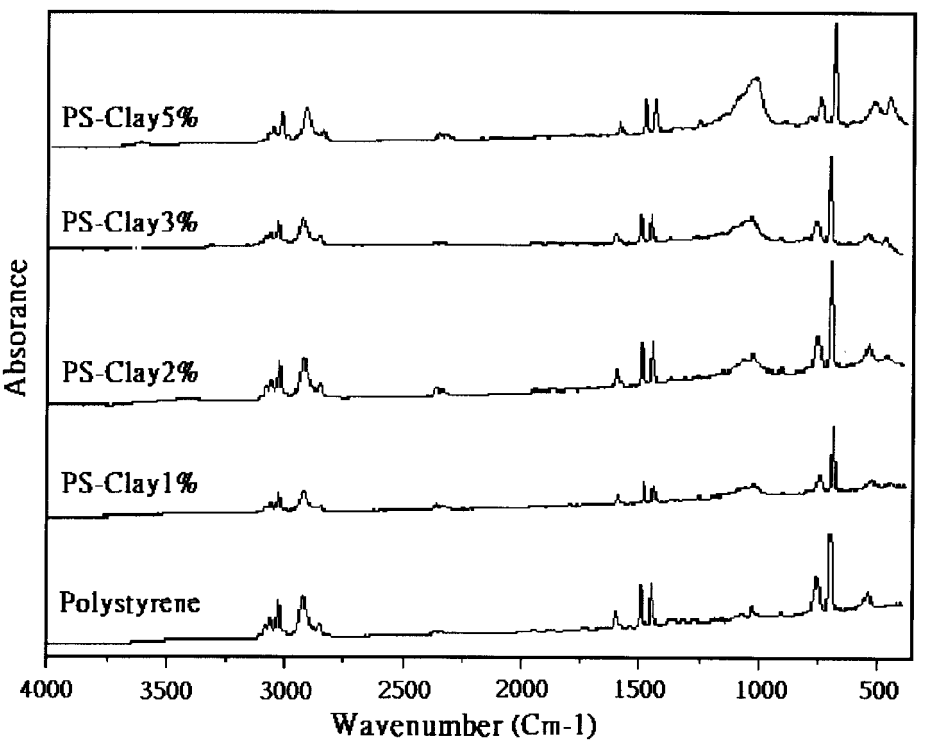

Figure 2 FTIR spectra of PS and a series of PsCN materials.

TABLE I
FTIR Band Assignments of PS and PsCN Materials

Frequency (cm^{-1})	Source	Assignment
3600+	MMT clay	Free H_2O
2900–3200	PS	Aromatic C—H
1600	PS	Aromatic C═C
1500	PS	Aromatic C═C
1450	PS	Aromatic C═C
1100	MMT clay	Si—O (stretching)
700	PS	Monosubstituted benzene
750	PS	Monosubstituted benzene
500+	MMT clay	Al—O (stretching)
400+	MMT clay	Mg—O

benzene), and 2900–3200 cm^{-1} (aromatic C—H), and those of MMT clay are shown at 1100 cm^{-1} (Si—O), 500+ cm^{-1} (Al—O), and 400+ cm^{-1} (Mg—O).[18] As the loading of MMT clay is increased, the intensities of the MMT clay bands become stronger in the FTIR spectra of the PsCN materials.

TEM

Figure 3 shows a TEM micrograph of the PsCN materials with 3 wt % clay loading. In this figure, the light regions represent PS, and the dark lines correspond to the silicate layers. The individual silicate layers are randomly distributed within the PS matrix. In addition, some larger intercalated layers can also be identified. The intercalation and exfoliation of the clay materials within the polymer matrix are demonstrated.

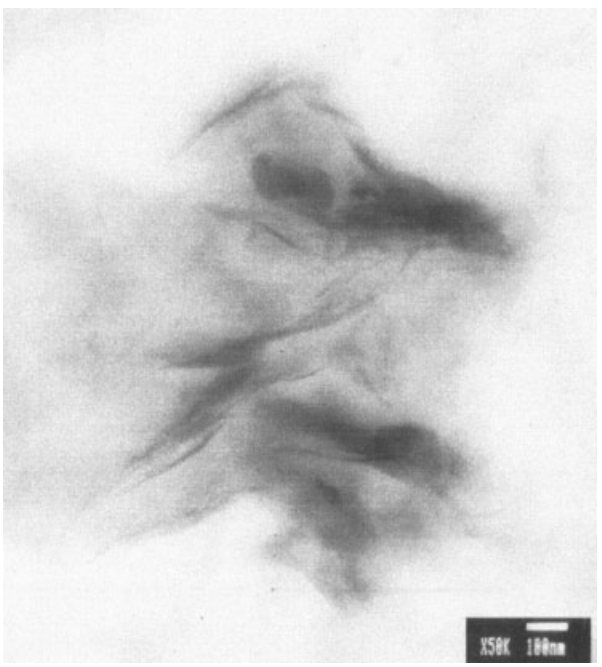

Figure 3 TEM micrograph of PS–clay 3%.

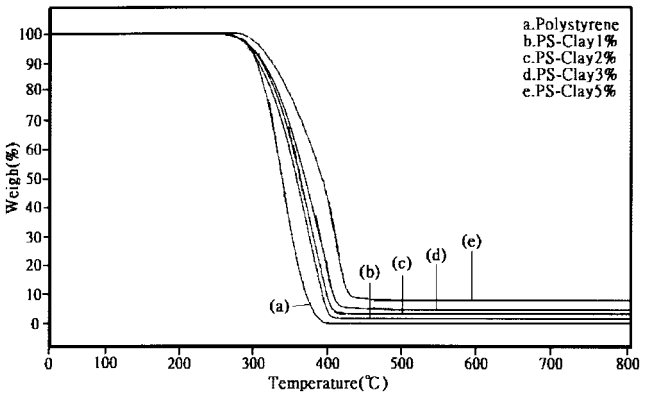

Figure 4 Thermal gravimetric curves of (a) PS, (b) PS–clay 1%, (c) PS–clay 2%, (d) PS–clay 3%, and (e) PS–clay 5%.

Thermal properties

The thermal decomposition behaviors of PS and a series of PsCN materials are given in Figure 4. In general, there appeared to be several stages of weight loss starting at ~300°C and ending at 800°C, which might be correspondent to the degradation of an intercalating agent followed by the structural decomposition of the polymers. In Figure 4(b–e), the onset decomposition temperatures of the PsCN materials are higher than that of pure PS and shifted toward higher temperature as the amount of Na^+–MMT increased. The onset decomposition temperatures for Figure 4(a–e) are approximately 306.7, 315.3, 322.0, 330.6, and 357.8°C, respectively. The nanocomposite with 5.0 wt % of clay shows a 50°C increase in the decomposition temperature than that of pure PS.[19] After ~500°C, the curves all became flat and the inorganic residue (i.e., Al_2O_3, MgO, SiO_2) mainly remained. The residual weights after complete decomposition are also ranked in order: 0.00, 1.44, 3.29, 5.19, and 8.27 wt % for Figure 4(a–e), respectively. It is clear that the PsCN materials improved the thermal stabilities due to the intercalated and exfoliated clay. The retarding effect of clay platelets on the decomposition of the polymer is obvious.

DSC thermograms for pure PS and a series of PsCN materials are shown in Figure 5. All samples were annealed at 150°C for a few minutes and then examined in the DSC. Pure PS exhibits an endothermic peak at approximately 100.9°C, corresponding to the glass transition temperature (T_g) of PS.[20] The T_g's for Figure 5(a–e) are approximately 100.9, 103.3, 104.5, 105.4, and 107.1°C, respectively. The T_g's of the PsCN materials are slightly higher than that of pure PS. This is tentatively attributed to the confinement of the intercalated

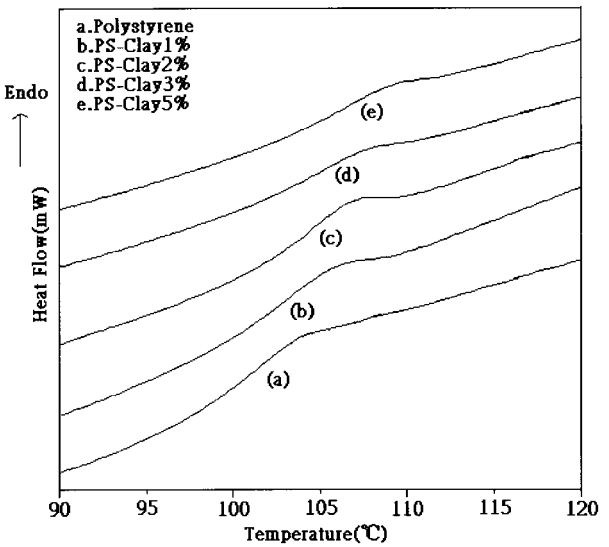

Figure 5 DSC thermograms of (a) PS, (b) PS–clay 1%, (c) PS–clay 2%, (d) PS–clay 3%, and (e) PS–clay 5%.

polymer chains within the clay galleries that prevents the segmental motions of the polymer chains.

Dielectric properties

As shown in Figure 6, the dielectric constant of PS is around 10–11 and slightly decreases as the temperature increases to 45°C and stabilizes to 70°C. As the amount of clay intercalated with PS increases, the composite materials show a decrease of the dielectric constant to less than 9 and a significant decrease of the dielectric loss to less than 0.1 (Fig. 7). Figure 7 shows that the dielectric loss decreases from 0.2 to 0.05 as the amount of intercalated clay increases from 0 to 5%. Figures 6 and 7 show the results taken from a frequency of 10 kHz. However, the magnitude of the decrease of the dielectric constant is much larger at low frequencies, as shown in Figure 8. Figure 8 shows the dielectric constant of the PsCN materials at various frequencies under 30°C. At a frequency of 120 Hz, the dielectric constant of PS is 25 and decreases to 12 by

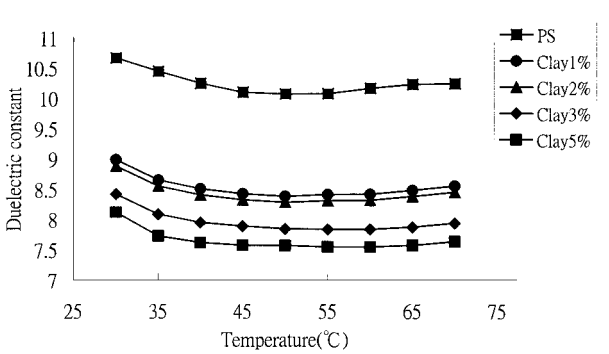

Figure 6 Dielectric constant of PsCNs at 10 kHz.

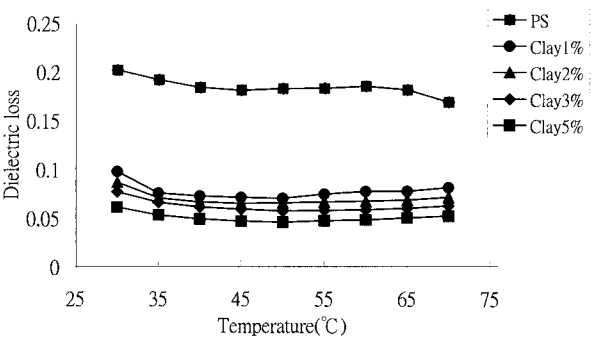

Figure 7 Dielectric loss of PsCNs at 10 kHz.

the addition of clay. As the frequency increases to 100 kHz, the dielectric constants of PS and the PsCN materials become closer, being 8.8–7.3, and decrease slightly according to the increasing amount of clay. It is well known that the polarization mechanisms in polymers are electronic, atomic, and dipolar orientation. The polarization contribution from the dipole orientation is dominated at low frequencies (<10 kHz). The decrease of the dielectric constant at low frequencies of the PsCN materials might be understood by that the exfoliated and intercalated clay within the polymer matrix has terminated the regular long chains of the polymer. The polymers become more random with shorter chains. The dipole orientation from the benzene side of PS may be constrained and not easily moved due to the confinement of the clay in nanoscale. The nanoscopic confinement effects from layered silicate inorganic hosts was also reported by Anastasiadis et al.[21] In their investigation, X-ray diffraction showed that the polymer is confined within 1.5–2.0 nm. This confinement effect is directly reflected on the local reorientational dynamics. We believed that the polarization of the dipole orientation is thus largely reduced due to this randomly distributed and confined structure.

CONCLUSIONS

A series of PsCN materials were synthesized by a free-radical polymerization process. The structures

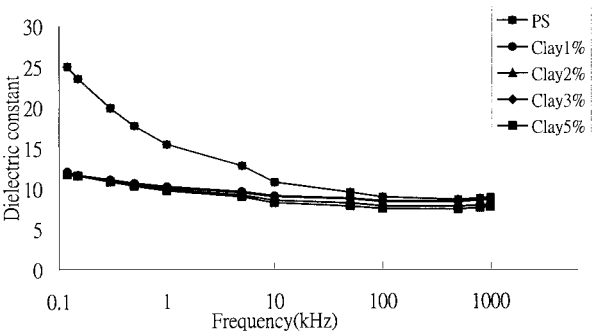

Figure 8 Dielectric constant of PsCNs at varies frequencies under 30°C.

were of intercalated and exfoliated forms and a mixture of both forms. A completely exfoliated structure results when the polymerization initiates in the gallery of the clay, which could be to 2 wt %. A mixture of intercalated and exfoliated structures were observed for more than 3 wt % clay. The as-synthesized PsCN materials were characterized by FTIR, XRD, TG/DSC, and TEM. Compared to the pure PS, the PsCN materials showed a higher T_g and a higher thermal degradation temperature. A decrease of the dielectric constant and low dielectric loss were observed for the PsCN materials. Especially, the dielectric constant at low frequency (<10 kHz) was completely suppressed. It is thought that the confinement effect of the intercalation process significantly suppressed the polarization of the dipole orientation at low frequency.

The financial support of this research by the NSC (91-2113-M-033-008) is gratefully acknowledged by the authors.

References

1. Kim, T. H.; Jang, L. W.; Lee, D. C.; Choi, H. J.; Jhon, M. S. Macromol Rapid Commun 2002, 23, 191.
2. Yeh, J.-M.; Liou, S.-J.; Lai, C.-Y.; Wu, P.-C. Chem Mater 2001, 13, 1131.
3. Yeh, J.-M.; Liou, S.-J.; Lai, C.-Y.; Wu, P.-C. Chem Mater 2002, 14, 154.
4. Strawhecker, K. E.; Manias, E. Chem Mater 2000, 12, 2943.
5. Kaviratna, P. D.; Pinnavaia, T. J.; Schroeder, P. A. J Phys Chem Solids 1996, 12, 1897.
6. Zhu, J.; Morgan, A. B.; Lamelas, F. J.; Wilkie, C. A. Chem Mater 2001, 13, 3774.
7. Kato, C.; Kuroda, K.; Takahara, H. Clay Clay Min 1981, 29, 294.
8. Kelly, P.; Moet, A.; Qutubuddin, S. J Mater Sci 1994, 29, 2274.
9. Akelah, A.; Kelly, P.; Qutubuddin, S.; Moet, A. Clay Min 1994, 29, 169.
10. Akelah, A.; Moet, A. J Mater Sci 1996, 31, 3189.
11. Akelah, A.; Moet, A. Mater Lett 1993, 18, 97.
12. Doh, J. G.; Cho, I. Polym Bull 1998, 41, 511.
13. Fu, X.; Qutubuddin, S. Mater Lett 2000, 42, 12.
14. Fu, X.; Qutubuddin, S. Polymer 2001, 42, 807.
15. Tseng, C.-R.; Wu, J.-Y.; Lee, H.-Y.; Chang, F.-C. J. Appl Polym Sci 2002, 85, 1370.
16. Tandon, R. P.; Mansingh, A.; Chandra, S. Synth Met 1999, 104, 137.
17. Liang, T.; Makia, Y.; Kimura, S. Polymer 2001, 42, 4867.
18. Chen, G.; Liu, S.; Chen, S.; Qi, Z. Macromol Chem Phys 2001, 202, 1189.
19. Kim, Y. K.; Choi, Y. S.; Wang, K. H.; Chung, I. J. Chem Mater 2002, 14, 4990.
20. Sikka, M.; Cerini, L. N.; Ghosh, S. S.; Winey, K. I. J Polym Sci Part B Polym Phys 1996, 34, 1443.
21. Anastasiadis, S. H.; Karatasos, K.; Vlachos, G.; Manias, E.; Giannelis, E. P. Phys Rev Lett 2000, 84, 915.